

High diagnostic performance of architectural distortion enhancement on CEM for predicting malignant breast lesions

Claudia B. Corona-Gonzalez^{1,2,a}, Beatriz E. Gonzalez-Ulloa^{1,b*}, David F. Perez-Montemayor^{2,3}, and Guillermo E. Juarez-Lopez⁴

¹Breast Imaging Department, Specialized Diagnostic Imaging Center, Zapopan, Jalisco; ²Centro de Imagenología Integral IMAX; ³Instituto de Estudios Superiores de Tamaulipas, Universidad Anahuac. Tampico, Tamaulipas; ⁴Centro de Estudios Especializados en Patología, Guadalajara, Jalisco. Mexico

ORCID: ^a0009-0002-5647-825X; ^b0009-0000-0042-0345

ABSTRACT

Introduction: The usefulness of contrast enhanced mammography (CEM) for assessing architectural distortion (AD) has not been defined. This study aimed to determine the diagnostic accuracy of AD enhancement on CEM for predicting malignancy and its histopathologic correlation. **Material and methods:** Patients with AD detected on 2D mammography, tomosynthesis (DBT), and/or ultrasound with BI-RADS categories 4 and 5 and supplementary evaluation with CEM were included. Histopathologic confirmation of the diagnosis or 24-month follow-up imaging studies to determine stability were reported. The risk of malignancy with AD enhancement was assessed with odds ratios (OR) with 95% confidence intervals (CI). Sensitivity, specificity, PPV, NPV, and accuracy of AD enhancement for predicting malignancy were calculated. **Results:** Forty-nine patients with 50 AD lesions (one patient had two AD lesions) were included. Twenty-nine (58.0%) were benign AD lesions, 5 (10.0%) were benign with upgrade potential (BWUP) lesions, and 16 (32.0%) were malignant. AD enhancement on CEM was observed in all breast malignancy cases ($n = 16$, 100%), compared to 12 (41.4%) of 29 benign ADs ($p < 0.001$). The risk of malignancy with AD enhancement on CEM was OR = 23.54 (95% CI, 2.77 to 199.9). AD enhancement on CEM had a sensitivity of 95.2% (95% CI, 76.2 to 99.9) and a specificity of 58.6% (95% CI 38.9 to 76.5) for predicting malignancy. The PPV was 69.7 (95% CI, 59.6 to 78.2), the NPV was 92.5% (95% CI, 63.9 to 98.8), and diagnostic accuracy was 76.9% (95% CI, 62.8 to 87.6). **Conclusion:** AD enhancement on CEM has high diagnostic accuracy for predicting breast malignancy. This study is the first in Mexico to present the experience with CEM in the evaluation of AD.

Keywords: Architectural distortion. Contrast enhanced mammography. Mammography. Ultrasound. Breast malignancy.

INTRODUCTION

Architectural distortion (AD) is the third most common abnormality detected on mammography¹. It is a parenchymal distortion without a visible mass seen on mammography as thin, straight lines or spiculations radiating from a point, with retraction, distortion, or focal rectification of the anterior or posterior margin of the breast parenchyma¹. With the advent of tomosynthesis (DBT),

more ADs have been detected. The primary causes of AD are breast cancer, radial scar, complex sclerosing lesion, adenosis, desmoid tumor, or diabetic mastopathy. Secondary causes are surgery and trauma².

Conventional breast imaging techniques such as mammography, DBT, ultrasound (US), or magnetic resonance imaging (MRI) have poor accuracy detecting malignant AD³⁻⁵. Contrast enhanced mammography (CEM), as a new imaging modality, has higher specificity

*Corresponding author:

Beatriz E. Gonzalez-Ulloa
E-mail: betyglez@yahoo.com

Received for publication: 24-04-2023

Accepted for publication: 29-05-2023

DOI: 10.24875/JMEXFRI.M23000053

Available online: 05-10-2023

J Mex Fed Radiol Imaging. 2023;2(3):172-183

www.JMeXFRI.com

2696-8444 / © 2023 Federación Mexicana de Radiología e Imagen, A.C. Published by Permanyer. This is an open access article under the CC BY-NC-ND (<https://creativecommons.org/licenses/by-nc-nd/4.0/>).

with similar sensitivity to MRI in diagnosing some breast pathologies since it allows evaluation of the morphology and physiological information of the lesion through contrast enhancement^{6,7}. The diagnostic performance of CEM has been compared with 2D mammography, tomosynthesis, and MRI in various scenarios as an alternative diagnostic imaging modality for patients not eligible for MRI, reassessment of response to neoadjuvant chemotherapy in high-and intermediate-risk patients, and evaluation of the extent of breast malignancy in patients with recently diagnosed cancer⁸⁻¹³. In addition, CEM offers advantages in terms of low cost and study duration¹⁴. As a cost-effective substitute, CEM can evaluate AD similarly to MRI providing a perfect correlation of mammographic and contrast-enhanced findings^{2,15,16}.

Breast cancer may manifest as AD, so biopsy is recommended¹⁷⁻¹⁹. CEM with AD enhancement can distinguish benign from malignant lesions^{20,21}. There is limited information on the behavior of AD enhancement in CEM and its association with breast malignancy^{2,17}. Our study aimed to determine the diagnostic accuracy of CEM in predicting malignant AD and its histopathological correlation.

MATERIAL AND METHODS

This cross-sectional study was conducted from December 2015 to December 2021 in the Breast Imaging Department at the Specialized Diagnostic Imaging Center in Zapopan, Jalisco, Mexico. Patients with AD detected on 2D mammography, DBT, and/or ultrasound with BI-RADS categories 4 and 5 were included. Patients with an unconfirmed histological diagnosis of AD or who did not complete the two-year follow-up period were excluded. Informed consent was not required for this retrospective analysis of data obtained in routine medical care. The study was approved by the Institutional Research Ethics Committee and the Research Committee.

Study development and variables

Patients were identified as having AD by mammography, DBT, and/or ultrasonography with supplemental evaluation by CEM. Histopathological confirmation of the diagnosis or a 24-month follow-up with imaging studies to determine lesion stability were reported. Age, sex, breast tissue composition according with American College of Radiology¹, and AD laterality were recorded.

Table 1. Breast AD diagnoses and their histopathologic confirmation or stability by imaging at 24-month follow-up

Benign breast AD	n (%)
Fibrocystic changes	4 (13.8)
Fibroadenomatoid changes	4 (13.8)
Radial scar	4 (13.8)
Sclerosing adenosis	3 (10.4)
Mature adipose tissue	1 (3.4)
Benign for stability ^a	13 (44.8)
Total	29 (100)
BWUP breast AD	n (%)
Atypical ductal hyperplasia	3 (60.0)
Atypical epithelial myoepithelial hyperplasia	1 (20.0)
Columnar cell change with atypia	1 (20.0)
Total	5 (100)
Malignant breast AD	n (%)
Invasive ductal carcinoma	13 (81.3)
Ductal carcinoma in situ	2 (12.5)
Phyllodes tumor	1 (6.2)
Total	16 (100)

^aIn 13 patients, the lesion was stable on breast US or mammography examinations at 24-months follow-up, and no biopsy was performed. AD: architectural distortion; US: ultrasound; BI-RADS: Breast Imaging Reporting and Data System; BWUP: benign with upgrade potential.

Protocol for image acquisition and analysis

CEM

Selenia Dimensions equipment (Hologic, Inc. Danbury, CT, USA) with 2D CEM imaging software (I-VIEW) was used. Urea and creatinine were verified as normal before the CEM examination. Informed consent was obtained for contrast agent administration. Images were obtained from Picture Archiving and Communication System (PACS) (Carestream™, Health Inc, version 12.1.5, Rochester, NY, USA).

A nonionic iodinated contrast medium (Ultravist 370, Bayer AG, Berlin, Germany) was used. The dose was 1.5 mL/kg intravenously with a dual injector (MEDRAD STELLANT DUAL, Bayer, Pharmaceuticals, Berlin, Germany) at 3.5 mL/sec with a maximum dose of 150 mL. Two minutes after the contrast injection, mammographic projections were started. Mediolateral oblique (MLO), craniocaudal (CC), and mediolateral

Table 2. CEM enhancement behavior in positive and negative mammography and ultrasound for detection of AD

Description	Positive mammography/ positive ultrasound	Positive mammography/ negative ultrasound	Negative mammography/ positive ultrasound	Total
Positive CEM ^a , n (%)	28 (84.8)	2 (25.0)	2 (22.3)	32 (64.0)
Negative CEM ^b , n (%)	5 (15.2)	6 (75.0)	7 (77.7)	18 (36.0)
Total, n (%)	33 (100)	8 (100)	9 (100)	50 (100)

^aPresence of enhancement of AD; ^bAbsence of enhancement of AD; AD: architectural distortion; CEM: contrast enhanced mammography.

Table 3. Characteristics of patients, BI-RADS categories and etiologic diagnoses of breast AD

Description	Total	%	Benign breast AD, n	%	BWUP breast AD, n	%	Malignant breast AD, n	%	p-value
Age, years, mean ± SD (min, med, max)	48.6 ± 9.8 (28, 48, 69)		49.3 ± 9.1 (28, 50, 67)		43.2 ± 3.1 (40, 43, 48)		48.9 ± 12.1 (30,47.5,69)		0.028
Sex									
Female	48	98.0	28	96.6	5	100	16	100	1.000
Male	1	2.0	1	3.4	0	0	0	0	
Total	49 ^a	100	29	100	5	100	16	100	
Breast composition									
Almost entirely fatty a	1	2.0	2	3.6	0	0	0	0	0.467
Scattered densities b	8	16.3	4	14.3	0	0	4	25.0	
Heterogeneous dense c	34	69.4	20	71.4	3	60.0	11	68.8	
Extremely dense d	6	12.3	3	10.7	2	40.0	1	6.2	
Total	49 ^a	100	29	100	5	100	16	100	
Laterality									
Right	20	40.0	12	41.4	2	40.0	6	37.5	0.950
Left	29	58.0	16	55.2	3	60.0	10	62.5	
Bilateral	1	2.0	1	3.4	0	0	0	0.0	
Total	50	100	29	100	5	100	16	100	
BI-RADS									
3	18	36.0	17	58.6	1	20.0	0	0	< 0.001
4	12	24.0	8	27.6	2	40.0	2	12.5	
5	20	40.0	4	13.8	2	40.0	14	87.5	
Total	50	100	29	100	5	100	16	100	

^a49 patients with 50 AD lesions (one patient had two ADs). AD: architectural distortion; BWUP: benign with upgrade potential; BI-RADS: Breast Imaging Reporting and Data System. SD: standard deviation; min: minimum value; med: median; max: maximum value.

(ML) views of the breast with the AD lesion were obtained first, followed by CC and MLO views of the contralateral breast and late projections, if necessary.

Projections were performed within 8 minutes according to standard protocols. Each image was obtained

simultaneously with low (26-30 kVp) and high energy (45-49 kVp) exposures. Recombined images were obtained with the algorithm of the mammography equipment to highlight the areas of iodinated contrast uptake.

Table 4. Comparison of characteristics of AD enhancement on CEM by diagnostic group

Description	Total, n	%	Benign breast AD, n	%	BWUP breast AD, n	%	Malignant breast AD, n	%	p-value
BPE									
Minimal	16	32.0	9	31.0	0	0	7	43.8	0.402
Mild	6	12.0	3	10.4	0	0	3	18.7	
Moderate	10	20.0	6	20.7	2	40.0	2	12.5	
Marked	18	36.0	11	37.9	3	60.0	4	25.0	
Total	50	100	29	100	5	100	16	100	
Enhancement									
Yes	32	64.0	12	41.4	4	80.0	16	100	< 0.001
No	18	36.0	17	58.6	1	20.0	0	0	
Total	50	100	29	100	5	100	16	100	
Internal enhancement pattern									
Homogeneous	5	15.6	1	8.3	2	50.0	2	12.5	0.327
Clumped	1	3.1	0	0.0	0	0	1	6.3	
Rim	1	3.1	1	8.3	0	0	0	0	
Heterogeneous	25	78.2	10	83.4	2	50.0	13	81.2	
Total	32 ^a	100	12	100	4	100	16	100	
Lesion conspicuity									
Low	7	21.9	3	25.0	2	50.0	2	12.4	0.521
Moderate	4	12.5	1	8.3	0	0	3	18.8	
High	21	65.6	8	66.7	2	50.0	11	68.8	
Total	32 ^a	100	12	100	4	100	16	100	

^a32 AD lesions with enhancement; AD: architectural distortion; BWUP: benign with upgrade potential; BPE: background parenchymal enhancement; BI-RADS: Breast Imaging Reporting and Data System; CEM: contrast enhanced mammography.

The recorded CEM descriptors²² were background parenchymal enhancement (BPE), categorized as: minimal, mild, moderate, or marked; the presence or absence of AD enhancement; the characteristics of the internal enhancement pattern: homogeneous, clumped, rim or heterogeneous; and the conspicuity of the lesion as low, moderate, or high. BI-RADS category 3, 4, or 5 was assigned based on the CEM findings and enhancement characteristics.

All CEM examinations were evaluated by the same breast radiologist (BGU) with 30 years of experience using a SecurView workstation (Hologic, Inc. Danbury, CT, USA) with 5 MP medical-grade monitors (BARCO, Kortrijk, Belgium).

Mammography and tomosynthesis

DBT in OML projections was performed in all patients referred for 2D mammography. In the case of AD detection, the CC projection was supplemented with DBT. DBT slices and synthesized images (images reconstructed with a lower radiation dose) acquired with Selenia Dimensions equipment (Hologic, Inc. Danbury, CT, USA) were analyzed.

Ultrasound

2D mammography or DBT and US were performed in all patients with AD with Acuson Antares or Acuson S2000 Evolution Helx equipment with touch control (Siemens, Erlangen, Germany). Multifrequency linear

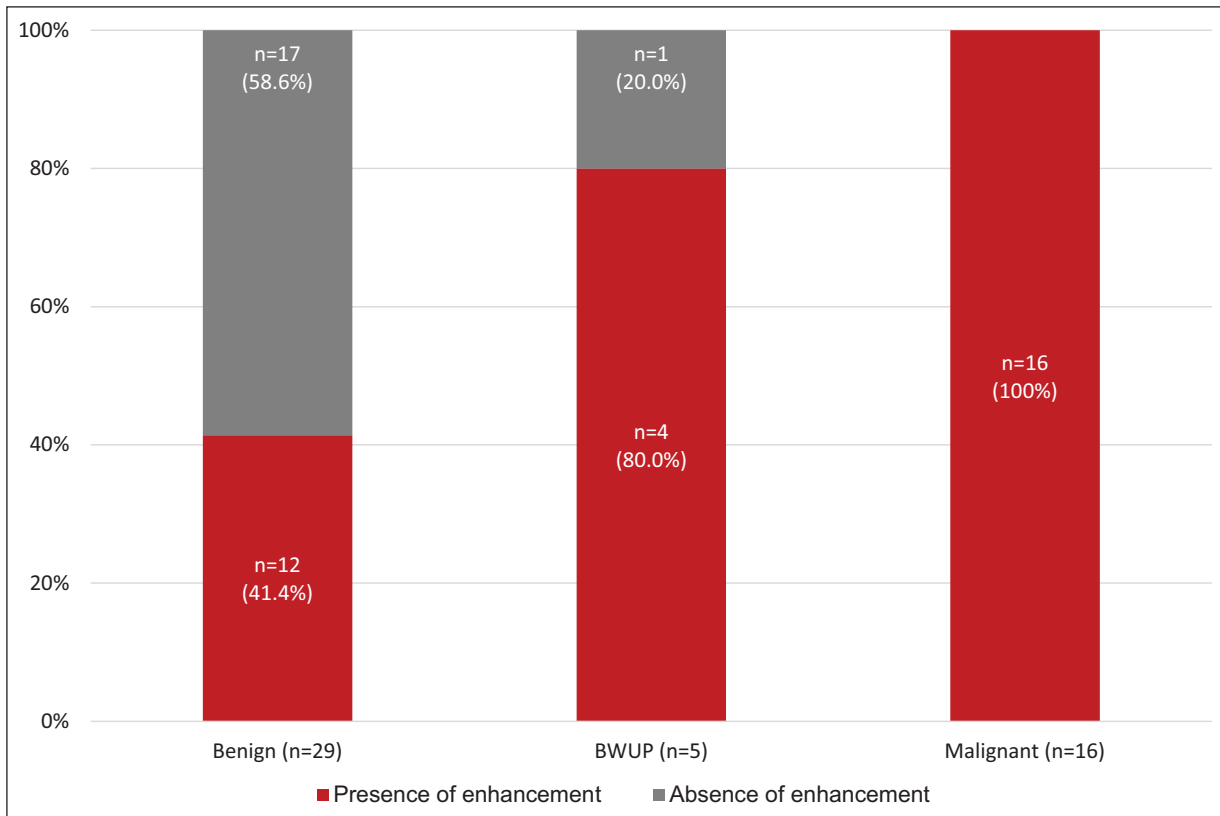


Figure 1. AD enhancement in CEM was present in all malignant AD lesions (n = 16, 100%), in contrast to 12 (41.4%) of the benign AD lesions (p < 0.001). BWUPs showed enhancement in 4 (80%) of 5 AD lesions.

AD: architectural distortion; CEM: contrast enhanced mammography.

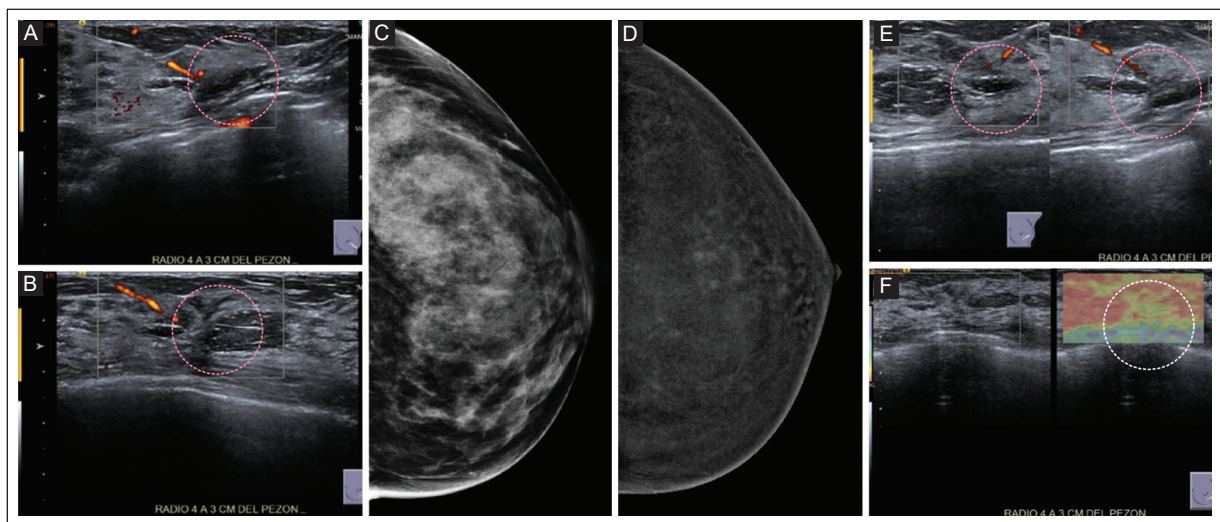


Figure 2. An asymptomatic 36-year-old woman. Grandmother with breast cancer. **A:** power Doppler US of the left breast, showing AD lesion, radial at 4 o'clock, 3 cm from the nipple with peripheral vascularity (circle). **B:** power Doppler US of left breast, showing AD lesion, antiradial, at 4 o'clock, 3 cm from nipple with peripheral vascularity (circle). **C:** CEM low energy of left CC image shows an extremely dense breast without abnormalities. **D:** CEM recombined of left CC view shows moderate background parenchymal enhancement. No abnormal enhancement in OLQ. **E:** power Doppler US of the left breast two years after CEM, radial and antiradial examinations show a less obvious AD lesion at 4 o'clock, 3 cm from the nipple with peripheral vascularity (circles). **F:** breast US with strain elastography two years after CEM shows soft AD (circle). Patient completed the 2-year follow-up period and was recategorized as BI-RADS 2.

AD: architectural distortion; CC: craniocaudal view; CEM: contrast enhanced mammography; OLQ: outer lower quadrant; US: ultrasound.

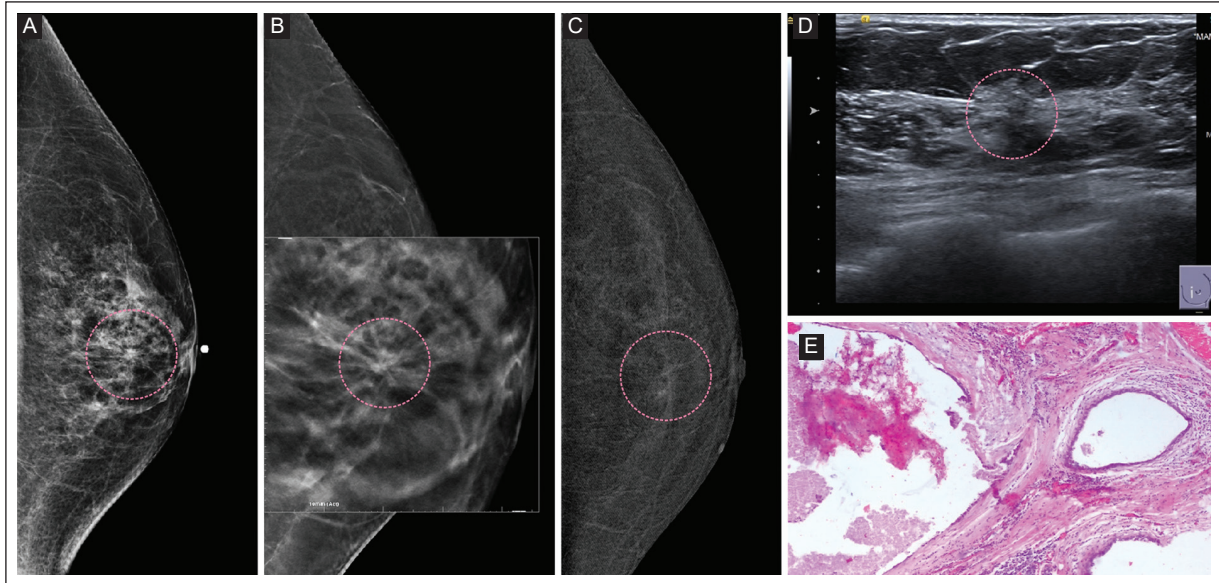


Figure 3. An asymptomatic 51-year-old woman. **A:** low energy CEM of left ML image with AD at 9 o'clock, middle third (circle). **B:** electronic magnification of DBT view of left breast showing AD with radiolucent center (circle). **C:** CEM recombined of left ML image showing mild background parenchymal enhancement. Heterogeneous, AD enhancement with low conspicuity and mammographic lesion partially enhanced (circle). **D:** grayscale breast US shows AD at 9 o'clock, 2 cm from the nipple, in the left breast (circle). **E:** these were biopsy-proven fibrocystic changes (H&E 10x). Breast tissue is identified with ducts with cystic dilations lined by simple cuboidal epithelium without atypia. A stroma with proliferation of collagen fibers and clusters of lymphocytes is also seen.

AD: architectural distortion; CEM: contrast enhanced mammography; H&E: hematoxylin and eosin; ML: middle lateral; US: ultrasound.

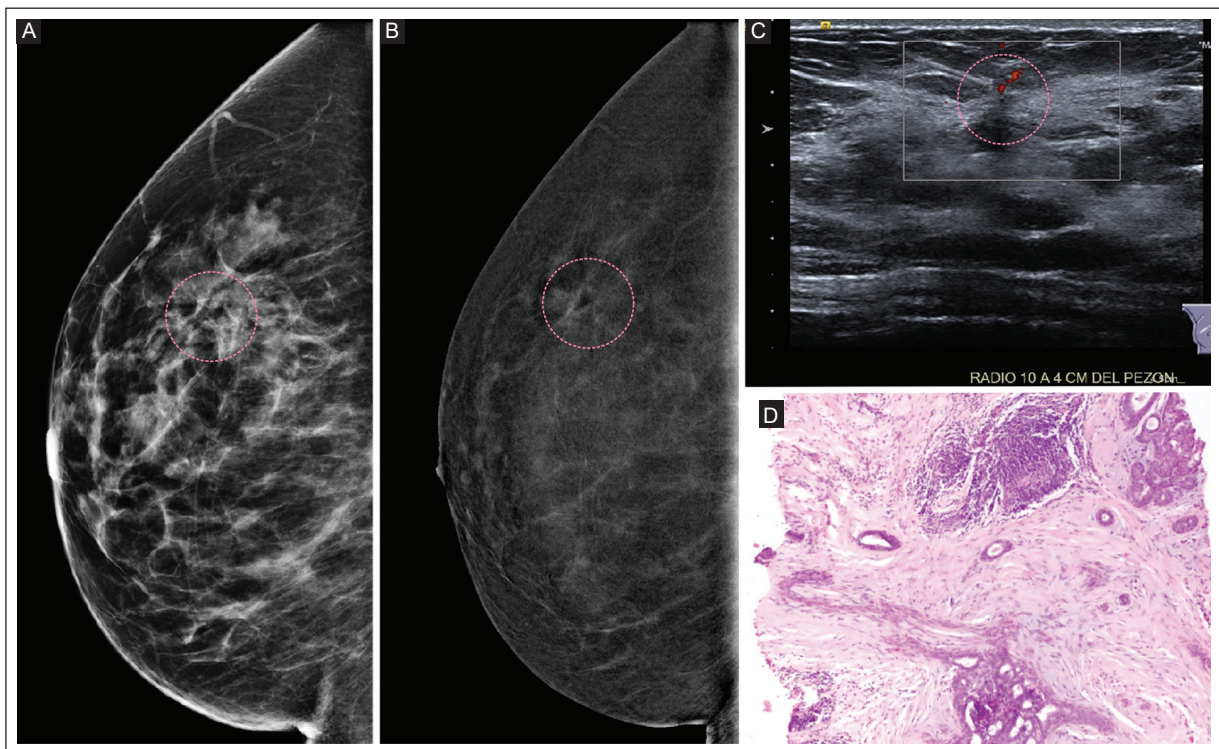


Figure 4. A 52-year-old woman with an AD in the right breast. **A:** CEM with low energy on right ML image showing AD in OUQ (circle). **B:** CEM recombined on right ML image shows moderate background parenchymal enhancement. Rim enhancement with low conspicuity and mammographic AD enhancement (circle). **C:** power Doppler US shows architectural distortion at 10 o'clock, 4 cm from the nipple with peripheral vascularity (circle). **D:** this was a biopsy-proven radial scar. Breast lesion with stratified ducts of epithelium converging toward the central portion, which is sclerotic (H&E 10x).

AD: architectural distortion; CEM: contrast enhanced mammography; H&E: hematoxylin and eosin; ML: middle lateral; OUQ: upper outer quadrant; US: ultrasound.

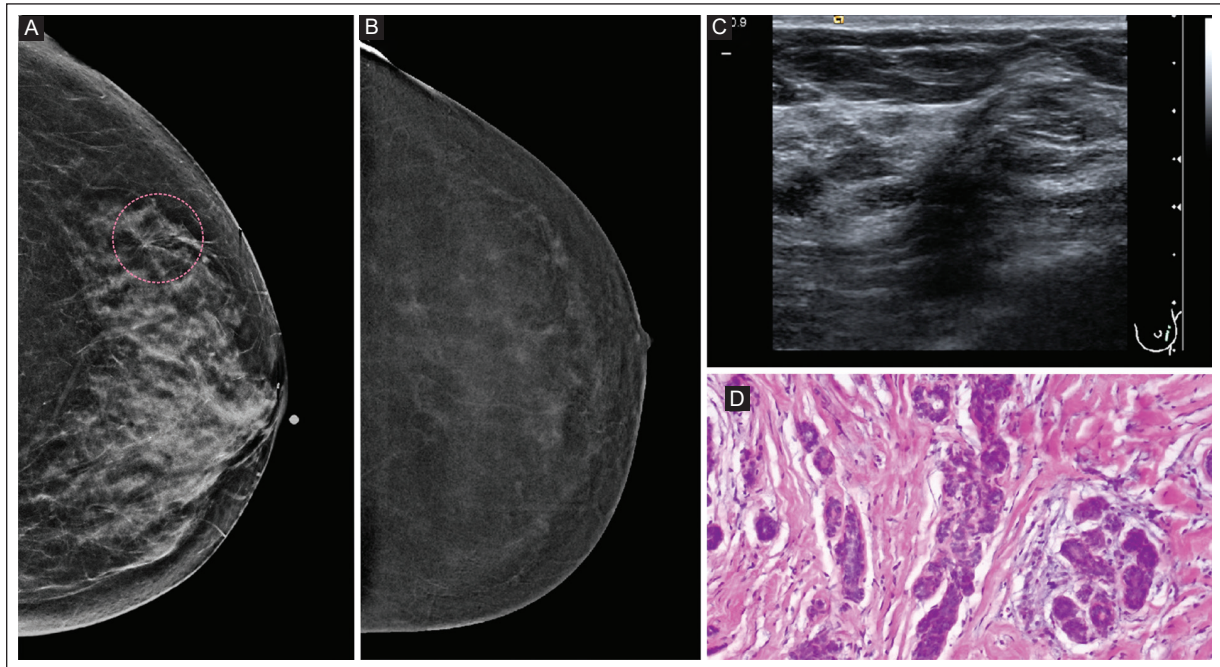


Figure 5. An asymptomatic 60-year-old woman. **A:** synthesized image of the left CC view shows a heterogeneous, dense breast with an AD in the middle third at 3 o'clock (circle). **B:** CEM recombined on left CC image shows mild background parenchymal enhancement and absence of the AD enhancement. **C:** grayscale US shows AD at 3 o'clock, 5 cm from the nipple, in the left breast. **D:** this was a biopsy-proven radial scar (H&E 40x). Proliferation of ducts completely lined with a bilayer of cells (myoepithelial and luminal) with usual hyperplasia without atypia or mitosis, embedded in a dense collagenous stroma, hyaline-paucicellular with fibrosis compressing the ducts. No malignant elements were found.

AD: architectural distortion; CEM: contrast enhanced mammography; CC: craniocaudal view; H&E: hematoxylin and eosin; US: ultrasound.

7.5-10 or 10-18 MHz transducers, respectively, were used. Grayscale ultrasound, color Doppler, power Doppler, and elastography were performed. Images were stored in a PACS.

Breast biopsy

An ultrasound-guided percutaneous Tru-cut biopsy was performed with a Magnum gun, 14G x 10 cm needle (Becton, Dickinson and Co. Franklin Lakes, NJ, USA). At least 5 cylinders were collected from all patients and stored in formalin. A single pathologist with 36 years of experience (GJL) performed the histopathological evaluation.

Statistical analysis

The mean, standard deviation, minimum, median, and maximum age were reported. Analysis of Variance (ANOVA) was calculated to compare the mean age between diagnoses of breast AD. Fisher's exact test compared the frequency of malignant AD and histopathologic confirmation. Sensitivity, specificity, positive predictive

value, negative predictive value, and accuracy for predicting malignant AD breast were determined. A p-value < 0.05 was considered significant. IBM-SPSS version 25 (IBM Co. Armonk, NY, USA) was used for data analysis.

RESULTS

AD was identified by mammography, DBT, and/or US in 57 patients. Seven (12.3%) patients were excluded. Three cases with AD enhancement on CEM had no histopathologic confirmation of the diagnosis, and 4 patients did not complete the 2-year follow-up period. No IV contrast reactions were reported. Fifty AD lesions in 49 patients (one patient had two ADs) were included.

Histopathologic diagnosis was confirmed in 36 (73.4%) of the 49 patients (Table 1), and 13 (26.6%) patients completed the 2-year follow-up period and were recategorized as BI-RADS 2. Twenty-nine (58.0%) of the 50 lesions were benign breast ADs, 5 (10.0%) were AD breast lesions with upgrade potential (BWUP), and 16 (32.0%) were malignant breast ADs.

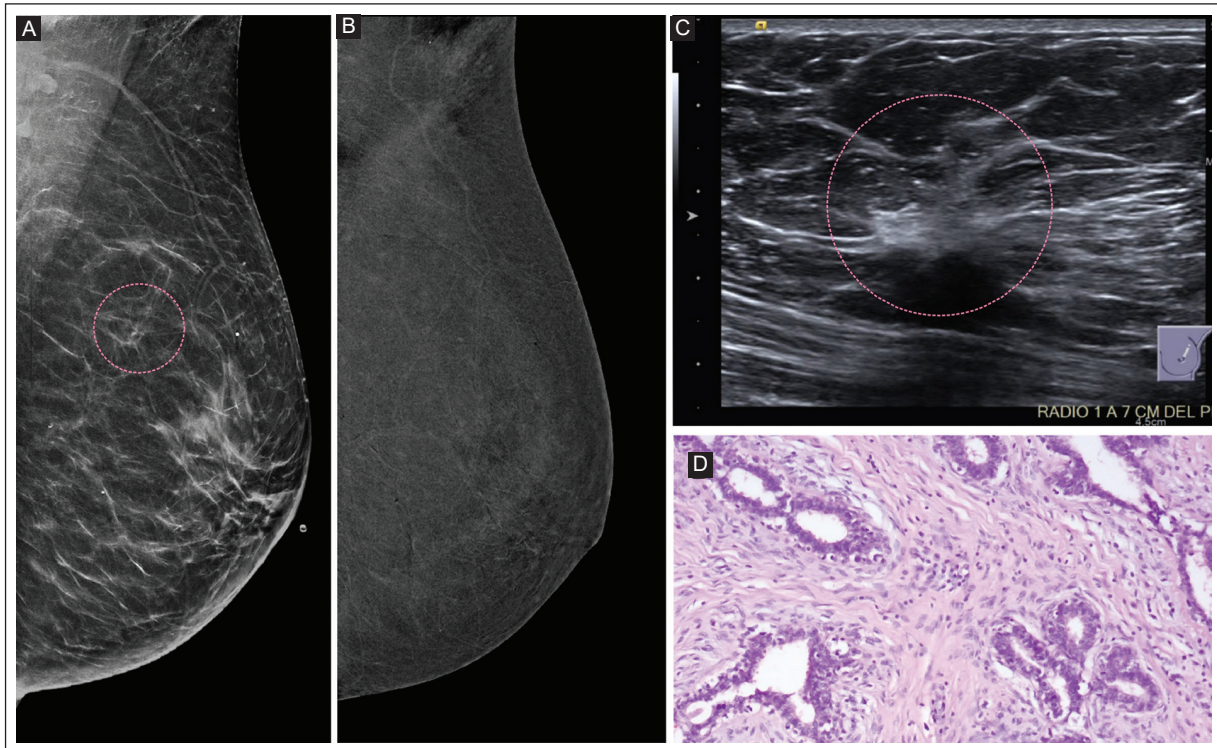


Figure 6. An asymptomatic 54-year-old woman with a history of right breast cancer 11 years ago. **A:** synthesized left MLO image shows scattered areas of fibroglandular density with subtle AD in the middle third of the OUQ (circle). Not seen on US. **B:** low energy CEM with AD lesion (image not shown). CEM recombined on left ML image shows minimal background parenchymal enhancement. No AD lesion enhancement. **C:** grayscale US breast one year after CEM showing interval change; AD lesion at 1 o'clock, 7 cm from the nipple of the left breast (circle). A breast biopsy was performed. **D:** this was a biopsy-proven fibroadenomatoid changes (H&E 40x). Breast parenchyma with ducts and lobules completely lined by a bilayer of cells (myoepithelial and luminal) with no significant cytologic changes embedded in a dense collagenous hypocellular stroma.

AD: architectural distortion; CEM: contrast enhanced mammography; H&E: hematoxylin and eosin; MLO: mediolateral oblique; OUQ: outer upper quadrant; US: ultrasound.

The detection of AD on mammography and US, associated with AD enhancement on CEM, is described in Table 2. AD enhancement was detected in 28 (84.8%) of 32 AD lesions found in mammography and ultrasound, while 7 (77.7%) of 9 AD lesions detected by ultrasound only did not show AD enhancement on CEM, the diagnosis was benign in six patients who completed the two-year stability period, and in another, the histopathological result was benign (mature adipose tissue). In two AD lesions detected by US showing AD enhancement on CEM, the diagnosis was ductal carcinoma in situ (DCIS) and a benign lesion (fibroadenomatoid changes) in another.

Table 3 shows the characteristics of the 48 women (98.0%) and one man (2.0%) included in the study. Age was comparable in patients with benign (49.3 ± 9.1 years) and malignant (48.9 ± 12.1 years) lesions, while patients with BWUP were significantly younger (43.2 ± 3.1 years) ($p < 0.028$). Heterogeneously dense breast tissue (c) according to ACR classification, was most

common in the three groups, with 71.4%, 60.0%, and 68.8% in benign, BWUP, and malignant lesions, respectively. AD was found more frequently in the left breast (benign 55.2%; BWUP 60.0%, and malignant 62.5%). There was a significant association between BI-RADS category 5 and the diagnosis of histopathologically-confirmed AD malignancy ($n = 14$, 87.5%) ($p < 0.001$).

Table 4 compares background parenchymal enhancement, the presence or absence of AD enhancement, the pattern of internal enhancement, and the conspicuity of the lesion in relation to the diagnosis of benign AD, BWUP AD, and malignant AD.

The presence of AD enhancement on CEM was observed in all cases with breast malignancy ($n = 16$, 100%) compared to 12 (41.4%) of 29 benign lesions ($p < 0.001$) (Figure 1). BWUP lesions showed AD enhancement in 4 (80.0%) of 5 lesions. The risk of malignancy associated with AD enhancement in CEM was OR = 23.54 (95% CI, 2.77 to 199.9).

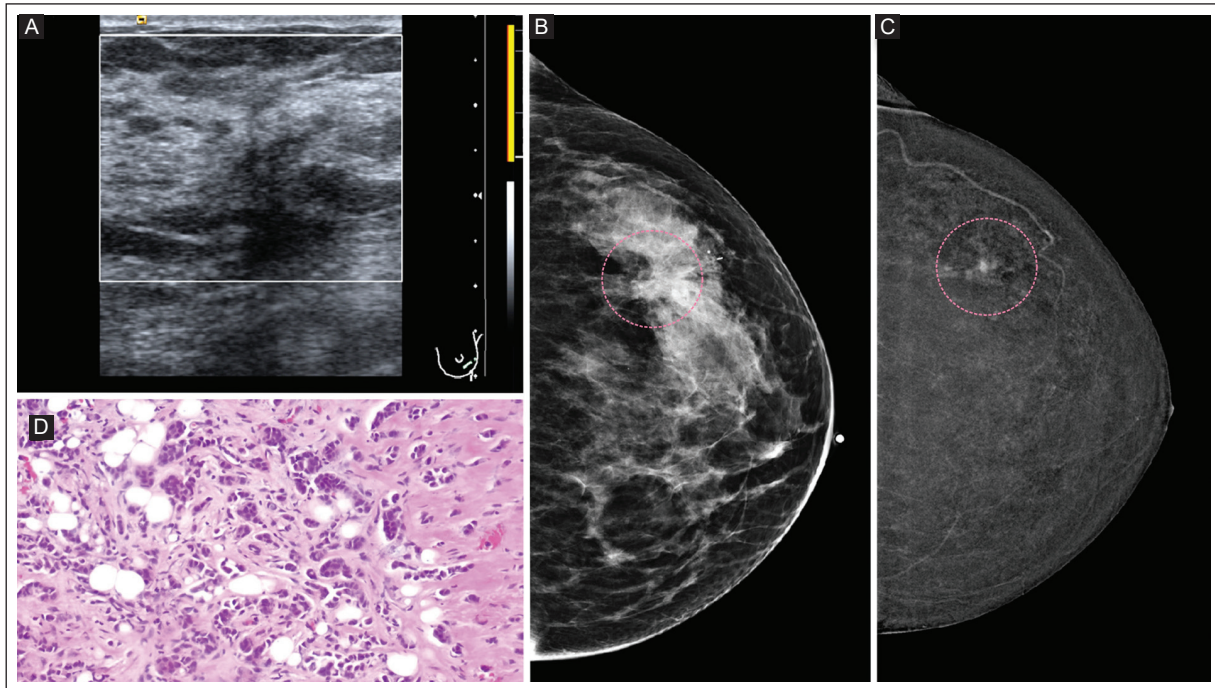


Figure 7. A 46-year-old woman with AD. **A:** power Doppler breast US showing avascular AD at 3-4 o'clock, 6 cm from the nipple in the left breast. **B:** low energy CEM of CC image shows heterogeneous dense breast with AD in OLQ (circle). **C:** CEM recombined of CC image shows mild background parenchymal enhancement. Focal, heterogeneous non-mass enhancement with high conspicuity and partial enhancement of mammographic AD lesion (circle). **D:** this was a CNB-proven invasive ductal carcinoma (H&E 40x). Breast tissue with evidence of epithelial malignancy consisting of elements with moderate pleomorphism. The cells are grouped together forming tubular structures and/or solid nests. The stroma with an intense desmoplastic reaction.

AD: architectural distortion; US: ultrasound; CEM: contrast enhanced mammography; CC: craniocaudal view; OLQ: outer lower quadrant; CNB: core needle biopsy; H&E: hematoxylin and eosin.

Figure 2 shows AD on US with peripheral vascularity and smooth on elastography that was not detected on mammography and CEM. AD was less evident on follow-up at 2 years with US, color Doppler, and elastography. The patient was recategorized as BI-RADS 2, and no biopsy was indicated. Figure 3 shows AD in the DBT view (radiolucent center) and US. On CEM, AD enhancement was observed in a patient with fibroadenomatoid changes. Figure 4 shows AD enhancement on CEM in a case with a radial scar. Figure 5 shows the absence of AD enhancement in the case of radial scar. Figure 6 shows the AD synthesized left MLO image not detected on US in a woman with a history of contralateral breast cancer. CEM showed no AD enhancement. A follow-up with grayscale US a year later showed an interval change with AD. The diagnosis was fibroadenomatoid changes. Figures 7 and 8 show the presence of AD enhancement in the CEM of two cases with malignant breast lesions.

The diagnostic performance of AD enhancement in CEM as a predictor of AD malignancy is shown in Table 5. The analysis included the 5 BWUP cases

because 80% of these lesions had AD enhancement. AD enhancement in CEM showed a sensitivity of 95.2% (95% CI, 76.3 to 99.9) and a specificity of 58.6% (95% CI 38.9 to 76.48) for predicting AD malignancy. The PPV was 69.7 (95% CI, 59.6 to 78.2), and the NPV was 92.5% (95% CI, 63.9 to 98.8). Diagnostic accuracy was 76.9% (95% CI, 62.8 to 87.6).

DISCUSSION

In this study, AD enhancement in CEM had a high diagnostic performance for predicting breast malignancy with high sensitivity and NPV. The risk of malignancy in the presence of AD enhancement was high (OR 23.54; 95% CI, 2.77 to 199.9). This study is the first in Mexico to present the experience with CEM in evaluating AD. Our results suggest that all AD lesions with enhancement on CEM would warrant biopsy or surgical excision for histopathologic confirmation.

A few papers have reported the usefulness of CEM in the diagnostic evaluation of AD. Patel et al.¹⁷, in a study of 45 patients with 49 ADs, demonstrated high

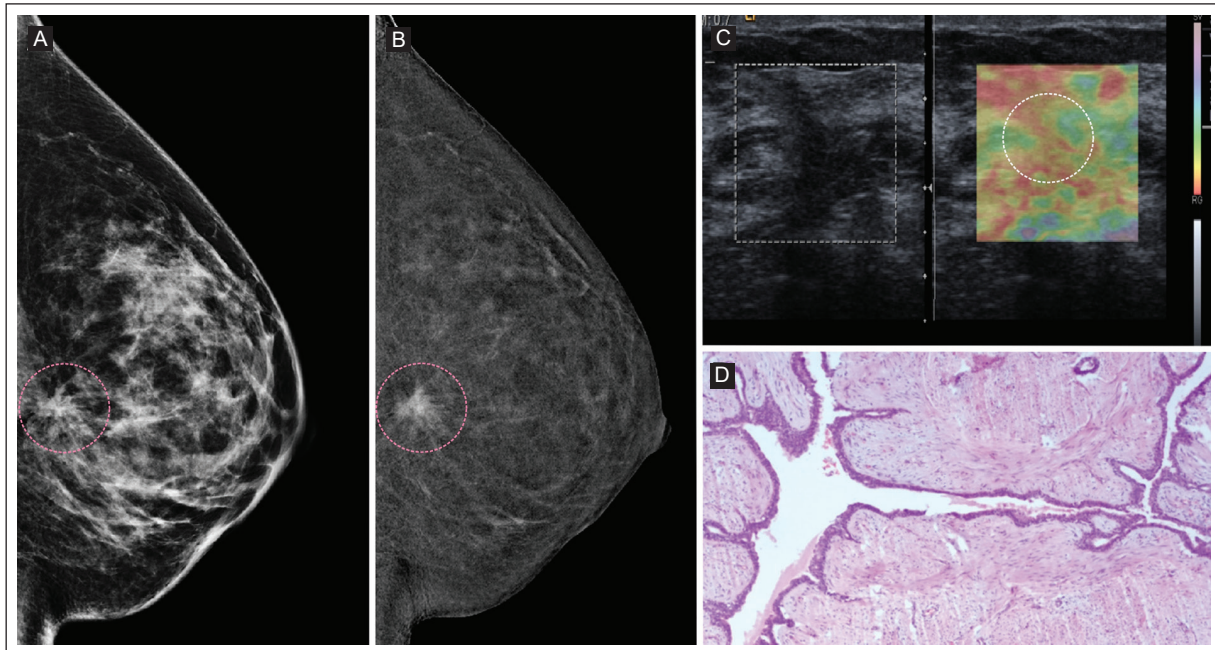


Figure 8. A 37-year-old woman with a palpable mass in the left breast. Her father with recently diagnosed breast cancer. **A:** low energy CEM image on left ML shows a heterogeneous dense breast with AD in posterior third at 6 o'clock (circle). **B:** CEM recombined on the ML image shows mild background parenchymal enhancement. Focal heterogeneous AD enhancement with high conspicuity and AD enhancement on mammography (circle). **C:** breast US with strain elastography shows hard AD (circle). **D:** this was a CNB-proven low-grade malignant phyllodes tumor (H&E 10x). Fibroepithelial breast neoplasm consisting of two components, the stroma with proliferation of spindle cells and mild atypia. The epithelial component consists of dilated ducts with double rows of epithelial cells.

AD: architectural distortion; CEM: contrast enhanced mammography; CNB: core needle biopsy; H&E: hematoxylin and eosin; ML: middle lateral; US: ultrasound.

Table 5. Diagnostic performance of AD enhancement on CEM for predicting breast malignancy

Parameter	%	95% CI
Sensitivity	95.2	76.2 to 99.9
Specificity	58.6	38.9 to 76.5
PPV	69.7	59.6 to 78.2
NPV	92.5	63.9 to 98.8
Accuracy	76.9	62.8 to 87.6

AD: architectural distortion; CEM: contrast enhanced mammography; PPV: positive predictive value; NPV: negative predictive value.

diagnostic accuracy of AD enhancement on CEM with a sensitivity of 96.7%, a specificity of 57.9%, an NPV of 91.7%, and an accuracy of 81.6% for the diagnosis of malignant AD. These results are similar to our study, which included 49 patients with 50 lesions. The sensitivity of AD enhancement was 95.2% and specificity 58.6%, with an NPV of 92.5% and an accuracy of 76.9% for predicting malignant breast AD. CEM may be a suitable alternative in the complementary diagnostic

evaluation of AD detected by US, mammography, and/or DBT. AD enhancement suggests malignancy, so a breast biopsy is recommended.

The findings of AD in CEM and their associated risk with malignancy were evaluated by Goh et al.² in a study of 700 CEM examinations with the development of a risk prediction model in 94 ADs detected with DBT in 92 patients (mean age, 52.4 ± 7.9 years). The diagnosis of breast malignancy was confirmed in 33 (35.1%). An associated risk of breast malignancy with AD was observed in the presence of marked enhancement (OR = 22.6; 95% CI 3.1-166.6) and spicule enhancement (OR 9.1; 95% CI 2.2-36.5). In our study, the presence of enhancement was confirmed in all 16 ADs with breast malignancy by histopathological examination. The risk association between AD enhancement in CEM and breast malignancy was high (OR = 23.54; 95% CI, 2.77 to 199.9). In contrast to Goh's study², we found no direct association between the magnitude of enhancement intensity and risk association with malignant AD. The high AD lesion conspicuity in our population study was comparable between benign ($n = 8$, 66.7%) and malignant lesions ($n = 11$, 68.8%) ($p < 0.521$). We found that an AD lesion

with enhancement of any intensity was associated with breast malignancy, regardless of whether the intensity was low, medium, or high.

ADs detected by mammography and US have a higher risk of malignancy. On the other hand, DBT-only AD has been reported to have a lower PPV for malignancy than mammographically detected AD². In contrast, the risk association with AD malignancy seen only on US is unknown. In our study, 7 (77.7%) of 9 ADs detected only by US showed no enhancement on CEM, and a benign AD lesion was diagnosed. Similarly, ADs detected only by mammography showed no enhancement on CEM. On the other hand, AD enhancement was found on CEM in 28 (84.8%) of the 33 ADs detected by mammography and US. ADs lesions detected with both imaging studies, US, and mammography, were more likely to have AD enhancement on CEM and a higher risk association for malignancy¹⁸.

The characteristics of AD in the CEM of BWUP lesions have not been described²³. In our study, 4 (80%) of 5 ADs with histopathological diagnosis of BWUP showed enhancement. In the context of BWUP lesions, the presence of AD enhancement on CEM suggests the potential for malignancy and the potential usefulness of CEM for early diagnosis when AD enhancement is detected and a breast biopsy is performed to confirm the diagnosis. Studies with larger numbers of patients with BWUP lesions are needed to characterize AD lesions on CEM.

This study's strength is characterizing the findings of ADs detected by mammography, DBT, and/or US and evaluated with CEM. Our results provide information on a topic that has been poorly explored. On the other hand, our study has some limitations related to the small number of study participants and the retrospective design in a single center. In addition, the subjective nature of the observer in assessing AD enhancement may reduce the accuracy of the result and increase inter-and intra-observer variability. The use of automated software to assess the presence and intensity of AD enhancement is desirable.

CONCLUSION

Our study found a high diagnostic performance of AD enhancement in CEM for predicting breast malignancy. A standardized lexicon of morphology descriptors, as offered in the first version of the BI-RADS[®] for CEM, may encourage consistent application of the lexicon to promote increased clarity and precision in reporting the

final CEM assessment²². Prospective multicenter studies with larger numbers of patients are needed to evaluate the diagnostic performance of CEM in AD.

Acknowledgments

The authors thank Professor Ana M. Contreras-Navarro for her guidance in preparing and writing this scientific paper. This original research was a thesis in the field of Radiology Specialty was awarded at the Primera Convocatoria Nacional 2023 "Las Mejores Tesis para Publicar en el JMeXFRI." Many thanks to Doctor Ignacio López-Mendez for his support in editing the figures.

Funding

This research received no external funding.

Conflicts of interest

The authors declare that they have no conflicts of interest.

Ethical disclosures

Protection of Individuals. This study complied with the Declaration of Helsinki (1964) and subsequent amendments.

Confidentiality of Data. The authors declare they followed their center's protocol for sharing patient data.

Right to privacy and informed consent. Informed consent was not required for this observational study of information collected during routine clinical care.

REFERENCES

1. D'Orsi C, Sickles EA, Mendelson EB, Morris EA. Breast Imaging Reporting and Data System: ACR BI-RADS[®] breast imaging atlas. 5th Edition. Reston: American College of Radiology, 2013.
2. Goh Y, Chan CW, Pillay P, Lee HS, Ben Pan H, Hung BH, et al. Architecture distortion score (ADS) in malignancy risk stratification of architecture distortion on contrast-enhanced digital mammography. *Eur J Radiol*. 2021;31(5):2657-2666. doi:0.1007/s00330-020-07395-3.
3. Durand MA, Wang S, Hooley RJ, Raghu M, Philpotts LE. Tomosynthesis-detected architectural distortion: Management algorithm with radiologic-pathologic correlation. *Radiographics*. 2016;36(2):311-321. doi:10.1148/rg.2016150093.
4. Shaheen R, Schimmelpenninck CA, Stoddart L, Raymond H, Slanetz PJ. Spectrum of Diseases Presenting as Architectural Distortion on Mammography: Multimodality Radiologic Imaging with Pathologic Correlation. *Semin Ultrasound CT MRI*. 2011;32(4):351-362. doi:10.1053/j.sult.2011.03.008.
5. Si L, Zhai R, Liu X, Yang K, Wang L, Jiang T. MRI in the differential diagnosis of primary architectural distortion detected by mammography. *Diagn Interv Radiol*. 2016;22(2):141-150. doi:10.5152/dir.2016.15017.
6. Dromain C, Thibault F, Diekmann F, Fallenberg EM, Jong RA, Koomen M, et al. Dual-energy contrast-enhanced digital mammography: Initial clinical results of a multireader, multicase study. *Breast Cancer Res*. 2012;14(3):R94. doi:10.1186/bcr3210.

7. Hobbs MM, Taylor DB, Buzynski S, Peake RE. Contrast-enhanced spectral mammography (CESM) and contrast enhanced MRI (CEMRI): patient preferences and tolerance. *J Med Imaging Radiat Oncol.* 2015;59(3):300-305. doi:10.1111/1754-9485.12296.
8. Lee-Felker SA, Tekchandani L, Thomas M, Gupta E, Andrews-Tang D, Roth A, et al. Newly diagnosed breast cancer: Comparison of contrast-enhanced spectral mammography and breast MR imaging in the evaluation of extent of disease. *Radiology.* 2017;285(2):389-400. doi:10.1148/radiol.2017161592.
9. Kim EY, Youn I, Lee KH, Yun JS, Park YL, Park CH, et al. Diagnostic value of contrast-enhanced digital mammography versus contrast-enhanced magnetic resonance imaging for the preoperative evaluation of breast cancer. *J Breast Cancer.* 2018;21(4):453-462. doi:10.4048/jbc.2018.21.e62.
10. Xing D, Lv Y, Sun B, Xie H, Dong J, Hao C, et al. Diagnostic Value of Contrast-Enhanced Spectral Mammography in Comparison to Magnetic Resonance Imaging in Breast Lesions. *J Comput Assist Tomogr.* 2019;43(2):245-251. doi:10.1097/RCT.0000000000000832.
11. Covington MF, Pizzitola VJ, Lorans R, Pockaj BA, Northfelt DW, Appleton CM, et al. The Future of Contrast-Enhanced Mammography. *AJR Am J Roentgenol.* 2018;210:292-300. doi:10.2214/AJR.17.18749.
12. Phillips J, Miller MM, Mehta TS, Zachary VF, Nathanson A, Hori W, et al. Contrast-enhanced spectral mammography (CESM) versus MRI in the high-risk screening setting: patient preferences and attitudes. *Clin Imaging.* 2017;42:193-197. doi:10.1016/j.clinimag.2016.12.011.
13. Francescone MA, Jochelson MS, Dershaw DD, Sung JS, Hughes MC, Zheng J, et al. Low energy mammogram obtained in contrast-enhanced digital mammography (CEDM) is comparable to routine full-field digital mammography (FFDM). *Eur J Radiol.* 2014;83(8):1350-1355. doi:10.1016/j.ejrad.2014.05.015.
14. Jochelson MS, Dershaw DD, Sung JS, Heerdt AS, Thornton C, Moskowitz CS, et al. Bilateral contrast-enhanced dual-energy digital mammography: Feasibility and comparison with conventional digital mammography and MR imaging in women with known breast carcinoma. *Radiology.* 2013;266(3):743-751. doi:10.1148/radiol.12121084.
15. Patel BK, Gray RJ, Pockaj BA. Potential cost savings of contrast-enhanced digital mammography. *AJR Am J Roentgenol.* 2017;208(6):W231-W237. doi:10.2214/AJR.16.17239.
16. Łuczyńska E, Heinze-Paluchowska S, Hendrick E, Dyczek S, Rys J, Herman K, et al. Comparison between breast MRI and contrast-enhanced spectral mammography. *Med Sci Monit.* 2015;21:1358-1367. doi:10.12659/MSM.893018.
17. Patel BK, Naylor ME, Kosiorek HE, Lopez-Alvarez YM, Miller AM, Pizzitola VJ, et al. Clinical utility of contrast-enhanced spectral mammography as an adjunct for tomosynthesis-detected architectural distortion. *Clin Imaging.* 2017;46:44-52. doi:10.1016/j.clinimag.2017.07.003.
18. Bahl M, Baker JA, Kinsey EN, Ghate SV. Architectural distortion on Mammography: Correlation With Pathologic Outcomes and Predictors of Malignancy. *AJR Am J Roentgenol.* 2015;205:1339-1345. doi:10.2214/AJR.15.14628.
19. Gaur S, Dialani V, Slanetz PJ, Eisenberg RL. Architectural Distortion of the Breast. *AJR Am J Roentgenol.* 2013;201:W662-W670. doi:10.2214/AJR.12.10153.
20. Kornecki A. Current Status of Contrast Enhanced Mammography: A Comprehensive Review. *Can Assoc Radiol J.* 2022;73(1):141-156. doi:10.1177/08465371211029047.
21. Chi X, Zhang L, Xing D, Gong P, Chen Q, Lv Y. Diagnostic value of the enhancement intensity and enhancement pattern of CESM to benign and malignant breast lesions. *Medicine (Baltimore).* 2020;99(37):e22097. doi:10.1097/MD.00000000000022097.
22. Lee C, Phillips J, Sung J, Lewin J, Newell M. Breast Imaging Reporting and Data System: ACR BI-RADS breast imaging atlas. Contrast Enhanced Mammography (CEM) (A supplement to ACR BI-RADS® Mammography 2013). 5th Edition. Reston: American College of Radiology, 2022.
23. Newell MS, Destounis S, Leung J, DeMartini W, Eby P. BI-RADS update: The edition formerly known as the 5th. Reston VA. USA. American College of Radiology (ACR); 2021.